International Journal of Biochemistry and Biophysics 10(2): 9-23, 2022 http://www.hrpub.org
DOI: 10.13189/ijbb.2022.100201

Evaluation of Phenol Sulfotransferase (SULT1A1) Ligand Binding Order

Joe D. Beckmann[1,*], Billie Schultz[1], Brian J. Doyle[2]

[1]Department of Chemistry, Alma College, 614 W. Superior St., Alma, MI, 48801, USA
[2]Department of Biology, Alma College, 614 W. Superior St., Alma, MI, 48801, USA

Received April 18, 2022; Revised May 28, 2022; Accepted June 27, 2022

Cite This Paper in the following Citation Styles

(a): *[1] Joe D. Beckmann, Billie Schultz, Brian J. Doyle , "Evaluation of Phenol Sulfotransferase (SULT1A1) Ligand Binding Order," International Journal of Biochemistry and Biophysics, Vol. 10, No. 2, pp. 9 - 23, 2022. DOI: 10.13189/ijbb.2022.100201.*

(b): *Joe D. Beckmann, Billie Schultz, Brian J. Doyle (2022). Evaluation of Phenol Sulfotransferase (SULT1A1) Ligand Binding Order. International Journal of Biochemistry and Biophysics, 10(2), 9 - 23. DOI: 10.13189/ijbb.2022.100201.*

Abstract Cytosolic sulfotransferases (SULTs) modify and regulate many endogenous and xenobiotic compounds. There are some disagreements regarding the binding pattern of their nucleotide (PAPS, PAP) and acceptor site ligands. Here we present an investigation of the homodimeric bovine phenol sulfotransferase (bSULT1A1) using several methods not dependent on catalytic turnover. Binding order was not determinable from intrinsic protein fluorescence changes in response to PAP(S), 7-hydroxycoumarin (7-HC) or pentachlorophenol (PCP). Equilibrium dialysis showed no binding of 7-HC to apo-bSULT1A1 up to 100 μM ligand, but inclusion of PAP induced biphasic binding of 7-HC. Isothermal titration calorimetry revealed exothermic half-sites binding of PAP to the dimeric protein. No binding of 7-HC to apo-SULT1A1 was detected, but SULT1A1:PAP also bound 7-HC at 0.5 per subunit. Differential scanning fluorimetry failed to show thermal stabilization of protein by excess 7-HC or PCP, whereas inclusion of PAP increased T_m dramatically. Susceptibility of bSULT1A1 to cleavage by chymotrypsin was not affected by excess 7-HC, but enzyme with PAP ± 7-HC resisted proteolysis. Excess 7-HC did not change protein cysteine reactivity with DTNB, whereas PAP impeded the fast phase of reaction attributable to C168. These observations indicate an ordered binding scheme for bSULT1A1. Testing other SULT ligand binding patterns with these methods is suggested.

Keywords Sulfotransferase, SULT1A1, Phenol, 7-Hydroxycoumarin, PAPS, Binding Order, Dialysis, Calorimetry, Kinetics, Proteolysis

1. Introduction

Sulfotransferases exist throughout biology [1,2]. They employ a common donor substrate, 3'-phosphoadenosine-5'-phosphosulfate (PAPS), and attach its sulfuryl group to hydroxyl or amine targets of a wide variety of acceptor substrates [3,4]. Vertebrates express members of the *SULT* gene super-family, the proteins usually being cytosolic homodimeric enzymes. A sequence-based nomenclature for these SULT enzymes is established [5], and members of the SULT1 group prefer phenolic acceptor substrates. SULT1A1 enzymes generally provide an inactivation or detoxification pathway due to enhanced solubilities of the sulfated products.

Structure determinations have propelled the understanding of SULT mechanisms. SULT1 acceptor substrate binding sites have abundant and variable hydrophobic residues that sample many positions [6], and this plasticity accommodates the spectrum of acceptor structures [7]. Computational methods have successfully predicted substrates and inhibitors [8-10]. The single PAP(S) binding site on each SULT subunit is relatively conserved. Most published structures include the reaction product nucleotide, adenosine-3', 5'-bisphosphate (PAP), which induces organization and more complete packing. Two independent teams reported structures of human

SULT1A3 [11,12], which preferentially sulfates catecholamines. Although both groups had included PAP, the initial crystals lacked nucleotide. Approximately 26% of residues could not be positioned, and Bidwell *et al*. [12] applied the descriptor of "intrinsically disordered". Both groups first suggested the possible roles of the disordered loops in substrate binding.

The dynamic loops, the tips of which converge in the closed conformation, are commonly annotated as L1-3. The largest of these, L3 (ca. F229-K258), folds onto both the PAP(S) and acceptor binding sites [13]. The primary points of L3 articulation are nearest to the PAP(S) binding site, and the interaction of the 3'-phosphate of PAP(S) with R257 may initiate closure of the loop. Modeling calculations indicated that L3 is not rigid, but at least flexes approximately midway during closure and/or opening [13]. Although it would seem that acceptor substrates would bind to the semi-open conformation during lid closure, it has been proposed that total closure of L3 leaves a pore through which smaller substrates are free to pass [13]. Thus, the position of L3, regulated by PAP(S) site occupancy, may adjust the size bias of acceptor substrate binding [13].

The role of SULT subunit dimerization is an ongoing question. A report of cooperative PAP(S)-dependent binding of pentachlorophenol (PCP) to the bovine SULT1A1 was interpreted as an evidence of subunit interactions [14], but binding of two equivalents of PCP per subunit might account for those observations. Fitting the complex inhibition of a SULT1A1 by palmitoyl-CoA invoked cooperative binding to the two subunits [15]. Clearer evidence of subunit interaction resulted from studies of PAP-dependent binding of 7-HC to bSULT1A1 [16]. The binding stoichiometries of 7-HC, PAP, and PCP all indicated "half sites" behavior, and so the models of SULT negative (anti) cooperativity and subunit oscillation during catalysis were first conceived. Others have since verified this anti-cooperativity by additional equilibrium titrations [17]. It is difficult, however, to envision much inter-subunit communication through the very limited SULT dimerization domain [18]. Future studies with engineered heterodimeric SULTs [19] will hopefully shed light on this issue.

A fundamental property of bi-substrate enzymes, which is potentially affected by quaternary structure, is ligand binding behavior and kinetic mechanism. Whether SULT ligand binding and catalysis follow a random or ordered pattern, with PAP(S) as the leading substrate, is not entirely clear despite numerous efforts at elucidating SULT mechanisms. Early work relied on initial rate kinetics analyses, which are difficult to interpret due to partial purification and enzyme heterogeneities. More satisfactory purifications emerged approximately forty years ago, and this was eventually followed by recombinant methods and complete isolations. While it is not possible to review all reports here, appreciate that the study of SULT kinetics has generated an array of models. Steady state kinetic studies of various SULTs have yielded both sequential ordered [15, 20-23] and random [24-28] mechanisms. Isotope exchange at equilibrium was thought to prove an ordered mechanism [29], but this has been criticized as overlooking the formation of dead end complexes within a random scheme [30]. Double inhibition kinetics measurements were consistent with an ordered mechanism that also revealed a significant interaction between the donor and acceptor binding sites [31]. Substrate trapping, however, indicated binding of acceptor substrate before PAPS, which is predicted by a random pattern [32]. Although kinetics approaches are historically valuable, analyses can be plagued by ambiguous parameters that emerge from a hypothetical model. Importantly, the ability of a model to fit a data set does not prove the model.

Therefore, we have endeavored here to evaluate ligand binding to bovine SULT1A1 by methods independent of catalytic turnover. This enzyme is a strong homolog of the human enzyme (83.7% identity, 94% similarity) [33,34], and so the current results are likely relevant to other members of this enzyme family.

2. Materials and Methods

2.1. Reagents and Enzymes

Buffers, salts, and PAGE reagents were from Fisher. 7-Hydroxycoumarin (7-HC, umbelliferone), PAP, PAPS, DTNB, papain, α-chymotrypsin, and PAGE molecular weight markers were from Sigma. Neutral protease was from Worthington, and pentachlorophenol (PCP) was from Aldrich. Sypro orange was from Invitrogen.

Recombinant bovine SULT1A1 devoid of fusion sequences was purified essentially as previously described [14,33,34]. *E. coli* DH5α was freshly transformed with pTrc99a(ΔlacI)::bSULT1A1, which requires no induction for high level expression. 1 L of well-aerated culture (14 h) in Terrific broth at 37 ℃ was chilled, centrifuged, and the pellets suspended in 100 mL Buffer A (20 mM Na-HEPES, 5 mM 2-mercaptoethanol, 0.5 mM EDTA, 10% (w/v) sucrose). After batch sonication for two minutes the sample was clarified by centrifugation. Soluble proteins were applied to Reactive Green agarose (Sigma, 2.5 x 18 cm), washed with 500 mL Buffer A/0.4 M NaCl, then the enzyme was eluted with Buffer A/2 M NaCl. After exhaustive dialysis against Buffer A, the sample was applied to DEAE cellulose (DE-52, Whatman), and eluted with a 1.5L linear gradient of Buffer A and Buffer A/0.4 M NaCl. Fractions with greatest SULT1A1 activity were evaluated by SDS-PAGE and Coomassie R-250 staining prior to pooling and concentration of the purest fractions. This was then passed over Sephadex G-200 (Sigma) in Buffer A/50 mM NaCl, followed by SDS-PAGE analysis to select fractions devoid of impurities as detectable by standard Coomassie R-250 staining. Such preparations commonly yielded 20-50 mg bSULT1A1 which can be stored as aliquots at -80 ℃ in either Buffer A/50 mM

NaCl/pH 7.4 or Buffer B (Tris-Cl instead of HEPES)/50 mM NaCl/pH 7.4 without loss of activity. No evidence of bound PAP [35] has been found after denaturation and TCA precipitation of the protein (not shown), thus ensuring that our experiments began with the apo-enzyme. Concentrations of SULT1A1 were determined using 280 nm absorbance and ε = 63.2/mM-cm, a value both calculated and verified [33].

2.2. Intrinsic Fluorescence Responses

The Aminco SLM 8000 spectrofluorimeter (excitation and emission wavelengths of 295 nm and 340 nm, respectively) was equipped with a cell holder maintained at 25 ℃ with a circulating water bath. Samples of 1.5 mL bSULT1A1 (0.50 μM subunits) in Buffer A/50mM NaCl were continuously stirred using a magnetic Teflon-coated plug. Experiments were also conducted using 50 mM sodium phosphate/pH 7.2 for comparison. Once signal was stabilized, the first ligand was injected (3-15 μL) using a Hamilton syringe through a narrow lid portal. After 100 sec the second ligand was delivered. Final concentrations are given in the figure legend (Fig. 1). Separate syringes were used for nucleotides vs. phenolic compounds. Emission intensities were continuously recorded at 1 sec intervals. A small buffer blank intensity was subtracted, then each trace was normalized to its own pre-injection intensity.

There was an apparent concentration-dependent drop of SULT1A1 emission in response to 7-HC injection (Fig. 1A, C). Such changes were also observed if the enzyme was denatured with 0.1% dodecyl sulfate. PCP also appeared to quench enzyme fluorescence (Fig. 1E), but this change was lost if 0.1% dodecyl sulfate was included.

2.3. Equilibrium Dialysis

Micro DispoDialyzer (#1356025, Spectrum) units, originally intended to float small sample volumes onto a large exchange reservoir, fit snugly into round bottom polypropylene cups obtained by cutting away the tops of common 12x75 mm tubes. The fluid volumes (50 μL inside the dialyzers, and 350 μL in the lower chambers) were chosen to equalize chamber levels. All experiments used Buffer B and were incubated at room temperature (24 ℃) for 4 h with occasional gentle agitation. Preliminary tests demonstrated this time are adequate for equilibration of free 7-HC across the membrane. Binding experiments used 9.3 μM SULT1A1 subunits inside the dialysis chambers and 0-100 μM 7-HC in the lower chambers. PAP was used at 15.4 μM when included.

Post-equilibration 7-HC concentrations were determined as follows. Aliquots of 40 μL from each chamber were combined with 0.25 M Tris-Cl pH 8.0/0.05% SDS/0.5X Buffer B, using volumes to achieve nominal [7-HC] of 1 μM or less. The denaturation released SULT-bound 7-HC, the increased pH ensured maximal detection sensitivity, and dilution ensured measurement by the DyNA Quant (Hoefer) fluorimeter within its linear response. Original concentrations were then calculated from the intensities, the known volumes, and by conservation of mass. All samples in replicate capillary cuvettes were measured at least twice for verification and averaging. All dialysis conditions reported here were repeated 6-20 times in order to gain statistical surety.

Binding of 7-HC in the presence of PAP was analyzed using the Scatchard plot. Standard errors for both axes (Fig. 1B) were calculated after application of propagation of errors through the calculations. The concavity of that plot indicated multiple 7-HC binding sites. Therefore, approaches to model the results were considered. The simplest scheme was a two-site model in which binding is predicted by Eq 1:

$$R = \{R_{max1}xC/(K_{d1} + C)\} + \{R_{max2}xC/(K_{d2} + C)\} \quad (1)$$

where R is the [7-HC] bound per SULT1A1 subunit, and C is the unbound [7-HC]. The right-hand terms of equation (1) were manipulated to form a single term, followed by moving the expanded denominator by cross-multiplication. Grouping terms by C^2, C and no C terms then set up a quadratic equation that yielded R/C = f(R) and the four binding parameters of (1). This was then used to model the experimental results and to estimate the K_d values for 7-HC binding. The values are not considered to be accurate, however, due to the greater complexity of the binding situation.

2.4. Isothermal Titration Calorimetry (ITC)

The VP-ITC instrument (Microcal, now owned by Malvern Panalytical) was operated by a personal computer with Origin software. The sample chamber (ca. 1.5 mL) maintained at 25 ℃ contained 10 μM bSULT1A1 samples in Buffer A/50 mM NaCl (A/50). The injection syringe containing A/50 buffer with 100-150 μM PAP or 100 μM 7-HC was constantly stirred at 260 rpm. Attempts to use much greater concentrations of either PAP or 7-HC were thwarted by excessive heats of dilution/mixing. Injection (4 μL) intervals of 120 sec ensured return to baseline. If the sample after a first titration remained clear, then the syringe was flushed and loaded with the second ligand for another titration. Such secondary runs were verified by loading the sample chamber with fresh SULT that was pre-incubated with the primary ligand, sometimes in much greater molar excess. Integrations of the exothermic signals generally required no baseline manipulation. Heats of injection at the ends of each titration were subtracted from the data, followed by Marquardt-Levenberg fitting to a simple single binding site model. Parameters of fit were ΔH, n, and K_a (inverted here to report K_d values). ΔS was then calculated. In all cases, 3-4 titrations were conducted from which averages and statistical errors were calculated (Table 1).

2.5. Differential Scanning Fluorimetry (DSF)

The procedure was essentially as previously described [33]. Triplicate 20 µL aliquots of 2.0 µM SULT1A1 subunits in Buffer B/50 mM NaCl/pH 7.4 containing 5X Sypro Orange (InVitrogen), ±10 µM PAP, ±10 µM pentachlorophenol (PCP), or ±200 µM 7-HC were ramped from 25 ℃ to 95 ℃ as the fluorescence of indicator dye was measured. Results were best displayed as incremental $\Delta F/\Delta T$ vs. T (approximate first derivative plots), which nicely reveals apparent melting point transitions (Fig. 5). Surprisingly, the SULT1A1+PAP samples had greatly elevated starting intensities that obscured the melting curves (not shown). Although the structure of Sypro orange is proprietary, we speculate that PAP induced its binding to the hydrophobic acceptor site of the enzyme.

2.6. Protease Sensitivity

α-Chymotrypsin (Sigma, TLCK treated) was dissolved at 1.0 mg/ml in 1.0 mM HCl/2.0 mM $CaCl_2$ and frozen in aliquots at -80 ℃. This was diluted just before use into Buffer B to make working stocks of 0.040, 0.020, and 0.010 mg/ml. bSULT1A1 was diluted in Buffer B to 0.25 mg/ml, followed by addition of buffer, PAP, and/or 7-HC to achieve 0.20 mg/ml (5.8 µM) SULT, ±50 µM PAP, ±50 µM 7-HC. After 10 minutes 20 µL aliquots of enzyme were delivered with mixing into 2.0 µL dilutions of protease. After an additional 30 minutes at ambient temperature each sample received 5.5 µL of Laemmli sample buffer [24], heated 3 mins at 95 ℃, centrifuged 30 sec, and subjected to SDS-PAGE (12% T gels). These were generally stained with Coomassie G-250 [25]. Band intensities were estimated using NIH Image analyses of images adjusted to exhibit grayscale variation that approximated what was visually apparent.

The results reported here were observed with two different preparations of bSULT1A1, and also by employing twice the concentrations of enzyme and ligands. Similarly designed experiments were conducted with papain and neutral protease (dispase).

2.7. Cysteine Reaction Kinetics

Purified SULT1A1 in Buffer B (220 µM, 400 µL) was exchanged into 50 mM NaPi/pH 6.5 by passage through a Sephadex G-50 column (1 x 20 cm). 2-Mercaptoethanol was thereby removed. Reactions of 0.80 mL at 25 ℃ were monitored at 412 and 600 nm using an HP 8452A spectrophotometer equipped with a thermostatted cuvette holder maintained at 25 ℃. Quartz semi-micro cuvettes initially contained 0.784 mL of nearly 10 µM SULT1A1 subunits and, if included, 60 µM PAP and/or 200 µM 7-HC. DTNB (5.0 mM, 16 µL) was introduced with quick mixing using a perforated enzyme spoon, thus achieving 100 µM reagent in the final reactions. A small subtractive correction (0.014) was made for the DTNB absorbance at 412 nm, and the 412-600 nm readings were then used for analyses. Although monitored for 500 sec, showing 300 sec allowed better display of the rapid phases of the reactions (Fig. 3). Control reactions of 2-mercaptoethanol with and without 60 µM PAP revealed no effect on the progress curve, which obeyed first-order kinetics. The reactions with SULT1A1 could not be fit, however, with a single first-order term as previously reported [26]. Progress curves without bound PAP were reasonably modeled using two first-order terms, whereas inclusion of PAP required three phases as shown by eq (2) below:

$$\Delta A_i = \Delta A_{max} - \Delta A_1 x e^{-k1t} - \Delta A_2 x e^{-k2t} - \Delta A_3 x e^{-k3t} \quad (2)$$

Fitting was achieved by either minimizing the sum of squared residuals or by the Marquardt-Levenberg algorithm within Origin software formatted with the above equation. We believe, however, that the derived rate constants are not entirely meaningful due to the complexity of the situation. For example, since binding of PAP affects the reactivity toward DTNB, it follows that cysteine modification will affect affinity for PAP. Since binding of PAP is reversible, DTNB reaction progress curves are unlikely to be due to a hypothetical fixed SULT1A1 conformation and cysteine exposure directed by pseudo first-order kinetics. Therefore, we have chosen to not provide the fitted parameters.

2.8. Molecular Modeling

Human SULT1A1 structures were previously used [12] to create the model of the bovine homolog, which is 83.7% identical and about 94% similar. Importantly, this build began with PDB 3u3o [27], which included PAP and *two* hydroxycoumarin ligands per subunit. Consequently, the structure is closed, or in a tight conformation, in which the ligand binding sites are covered by three surface loops. L1 (E83-T91) and L2 (H141-F158) are most closely juxtaposed to the phenolic acceptor binding domain, and L3 (F229-K258) is the more extensive lid that covers both the phenol and nucleotide binding domains. Direct evidence of L3 mobility dates back to the structural determinations of human SULT1A3 which unintentionally lacked ligands [13,14]. Movements of L1-3 have been studied by sophisticated computational methods [28].

For this work L1-3 were manually pivoted using Swiss PDB Viewer. The torsion tool was used to rotate phi and/or psi dihedral angles of a selected residue near the border of a loop. Coordinate changes were directed across the loop, with the extent of consequential movement limited by temporarily breaking a peptide bond near the opposing loop border. Such pairs were accepted if torsion adjustment kept the broken peptide nitrogen and carbonyl groups in reasonable proximity, thus allowing re-ligation. The pairs of torsioned phi/psi residues-toward-peptide bonds used to create the opened bSULT1A1 model (Fig. 4) are as follows. For L1: T91->L82/E83. For L2: R144->G153/T154, R144->T154/W155, R144-> D156/S157. For L3: F229->R257/K258, M256-> N239/Y240, S253->T238/N239, G259->S228/F229.

Both the original (closed) and modified (open) models were then examined for steric clashes. PDB Viewer easily selected either inter-side chain or side chain-to-backbone clashes, followed by testing a library of common side chain rotamers to minimize such repulsions. The only noteworthy clash was observed between the side chain of A86 and the outer, or second, bound hydroxycoumarin in the modified (open) model.

Both models were finally scrutinized using the PDB Viewer Ramachandran analysis of phi/psi angles. The original (closed) published structure presented four residues (G17, G50, G153, G170) slightly outside of the generally allowed plot zones. Similar occurrences of these glycine counterparts in other SULT structures were found. Our new (open) model presented two additional residues (T91 and F229) on the edge of allowed phi/psi pairings. Note that these were used in part to open L1 and L3, respectively. The deviation suggests that these loops may exist in a slightly higher potential energy state in the open configuration, thus favoring closure as the ligands dock to form the tight conformation.

Swiss PDB Viewer fortunately saves modified coordinates in PDB format, thus allowing the use of other programs (MacPyMol) with finer display options to render figures for presentation (Fig. 4).

2.9. Steady State Kinetics Analyses

Re-analyses of our previously published catalytic data [12] were performed using Origin software formatted with the following steady state ordered bi-substrate equation (3) [29]:

$$v/E = \{TN \times A \times B\} / \{K_{ia} \times K_{mB} + K_{mB} \times A + K_{mA} \times B + AxB\} \quad (3)$$

where E = SULT subunit concentration, $TN = V_{max}/E = k_{cat}$, A is [PAPS], B is [7-HC], K_{ia} is the dissociation constant for PAPS, and K_m terms are the values for the two substrates. Fitting by the Marquardt-Levenberg algorithm only required 7-19 rounds of calculations to converge on best fits, depending on assumed initial estimates. In contrast, fitting the same data according to a random kinetic scheme [12] required about 76-169 iterations to complete the fitting using the same initial estimates as used for the ordered calculations. In addition, the reduced chi-square parameters with the ordered model were 25-30% less than obtained with the random scheme.

3. Results

3.1. Intrinsic Fluorescence Responses

Tryptophanyl fluorescence is often responsive to protein structural changes induced by ligand binding, and so the responses of the bovine SULT1A1 to several ligands was measured (Fig. 1). Initial additions of excess 7-HC or PAP alone had little impact on enzyme fluorescence (Fig. 1A and B, respectively). However, subsequent additions of PAP or 7-HC immediately quenched about 20% of the emission in both cases. These changes required both ligands, and so it is not possible to conclude from these results alone whether their binding is ordered or random. The 3-5% drop in bSULT1A1 fluorescence upon addition of 7-HC only (Fig. 1A, C) initially suggested its binding, and this fractional change gradually declined with subsequent additions in a manner consistent with a binding titration (not shown). However, the same result occurred if the enzyme was denatured with 0.1% dodecyl sulfate (not shown) and thus unable to meaningfully bind 7-HC. The UV absorbance spectrum of 7-HC overlaps with both the excitation and emission wavelengths used in this experiment. Therefore, 7-HC created inner filter effects that would lead to incorrect conclusions regarding its binding to bSULT1A1.

PAPS was then used as the nucleotide (Fig. 1C, D). Again, there was no appreciable response of protein emission to nucleotide alone, but secondary addition of 7-HC triggered a rapid decline of bSULT1A1 intensity. The slower rebound was due to sulfation of 7-HC, dissociation of 7-HC-sulfate, and return of protein structure to a nucleotide-bound state.

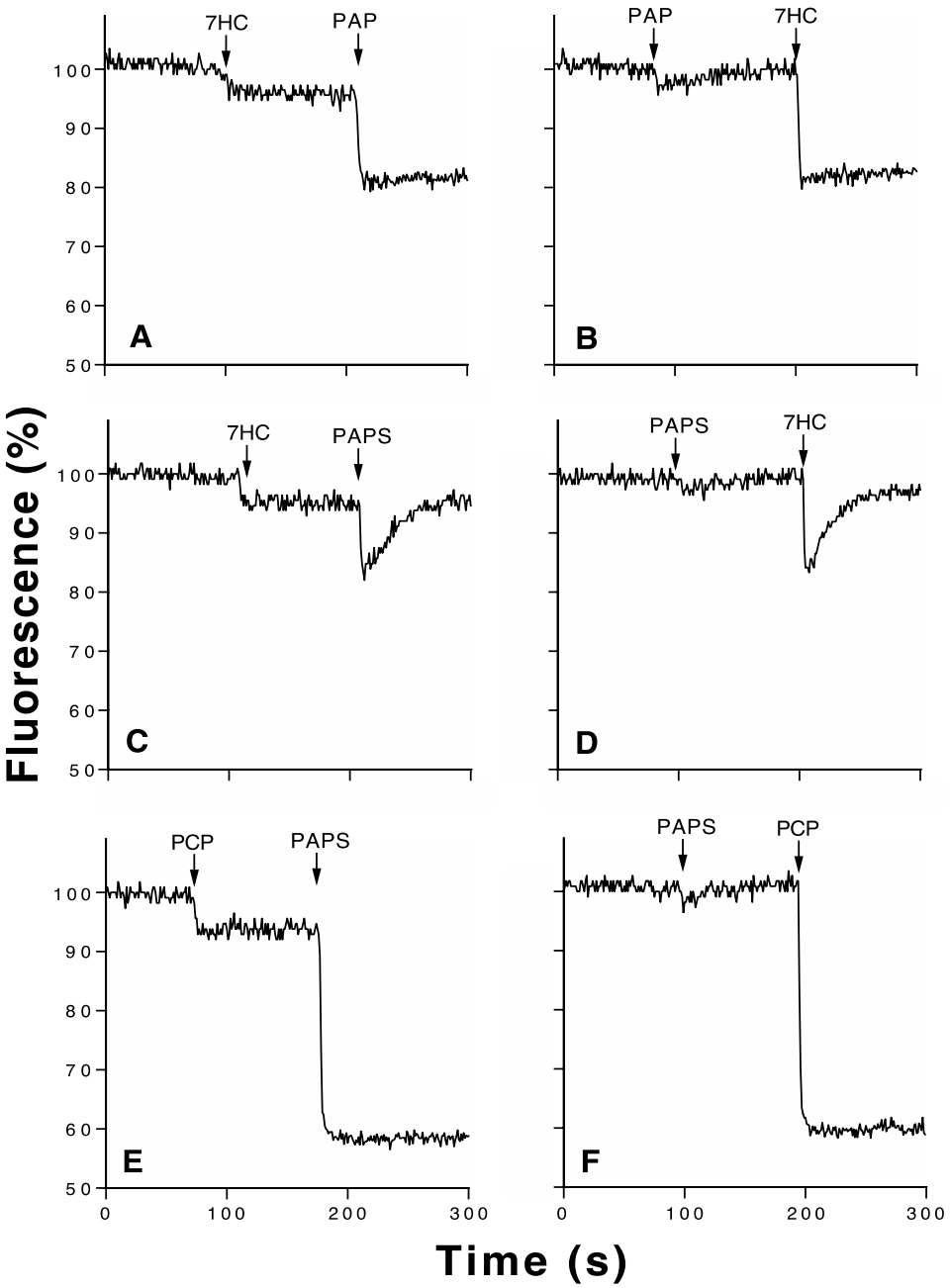

Figure 1. Responses of bSULT1A1 protein fluorescence to ligands. Each panel is scaled equally for both time and intensity, the latter being normalized to its own pre-injection value. Stirred 1.5 mL samples at 25 ℃ began with 0.50 μM enzyme subunits in Buffer A/50 mM NaCl (*Methods*). PAP or PAPS injections resulted in 5.0 μM nucleotides, and 7-HC or PCP injections produced 1.0 μM ligands. Note that the 3-4% drops in response to 7-HC only (A, C) are an inner filter effect artifact (see *Results*).

A third set of experiments (Fig. 1E, F) tested PAPS and PCP, a very potent SULT1 inhibitor [14,42]. Initial injection of PCP caused a small 7-8% drop of protein fluorescence (Fig. 1E). This was abolished by SDS (not shown), thereby indicating the effect was due to ligand binding rather than an inner filter artifact. Subsequent addition of PAPS induced an immediate 40% drop of SULT1A1 emission (Fig. 1E), which is the maximum amount of quenching by PCP previously reported [14]. This same degree of intensity drop occurred in response to PCP addition subsequent to injection of PAPS (Fig. 1F). In contrast to what was observed with 7-HC, the drop of intensity was stable owing to the inhibitory property of PCP.

It was hoped that these experiments would reveal either ordered or random binding of PAP(S) and 7-HC to bSULT1A1. However, the results only indicated that the protein structural changes behind the drop in tryptophanyl fluorescence required binding of both ligands. Additional methods were needed to evaluate bSULT1A1 ligand binding details.

3.2. Equilibrium Dialysis

The sensitivity of 7-HC fluorescence detection allowed measurement of its binding to SULT1A1 by equilibrium dialysis (Fig. 2). No binding occurred without PAP (Fig. 2A) up to 100 µM 7-HC. However, inclusion of the nucleotide stimulated saturable binding of 7-HC. The Scatchard plot (Fig. 2B) curvature revealed multiple affinities governing this binding, and modeling (Methods) those results was achieved with K_d values of 0.70 and 40 µM. The initial higher affinity binding phase suggested a stoichiometry of 0.5 7-HC per subunit, or a single 7-HC/SULT dimer. The lower affinity binding was consistent with two 7-HC per subunit, which has been observed with a human SULT1A1 structure [27].

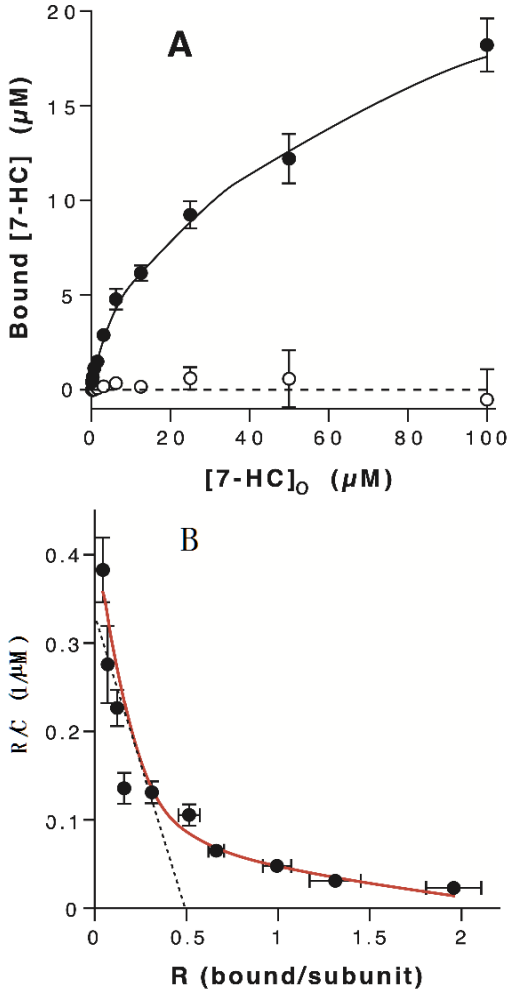

Figure 2. Equilibrium dialysis of SULT1A1 against 7-HC. The direct plot (panel A) are responses without (*open circles*) or with (*closed circles*) 15.4 µM PAP. $[7\text{-HC}]_o$ are initial values in the lower chambers, with 9.3 µM SULT1A1 in the upper compartment (see Methods). The Scatchard replot (panel B) uses the ratio approach of R being bound 7-HC/SULT1A1 subunit and C being non-bound (free) [7-HC]. The curve in the replot was calculated using a two sites model and K_d values of 0.7 and 40 µM (Methods). Symbols cover the standard errors unless indicated otherwise.

3.3. Titration Microcalorimetry

ITC measures enthalpic changes that often accompany the binding of ligands to a receptor. Titration data are numerically fit to models that then reveal ΔH, binding stoichiometry and affinity constants. The ΔG is directly obtained from K_a, then ΔS of binding is calculated. Representative fitted titrations are shown in Fig. 3, with Table 1 summarizing the thermodynamic parameters from many such experiments.

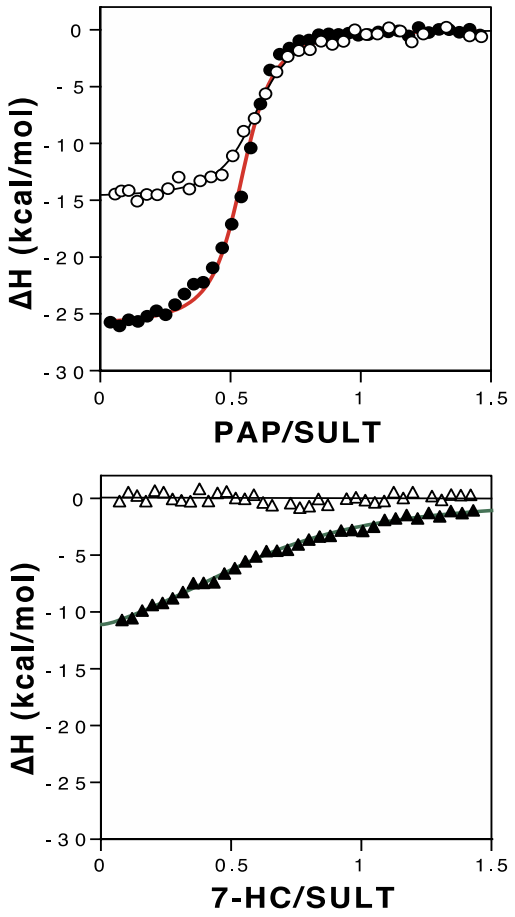

Figure 3. Isothermal titration calorimetry of SULT1A1 with PAP and 7-HC. The *open symbols* are from titrating PAP (upper panel) and 7-HC (lower panel) into 10 µM apo-enzyme (no 7-HC or PAP, respectively). The *closed symbols* are titrations into enzyme plus the second ligand (15 µM). The smooth curves are numerical fits for a single binding site. See Table 1 for a compilation of the resulting thermodynamic parameters.

Whereas the apo enzyme titrated with PAP generated a robust exothermic signal (Fig.3, *open circles*), no signal was observed from its titration with 7-HC (*open triangles*). Since the inclusion of excess PAP before initiating 7-HC titration *did* produce an exothermic profile (Fig. 2, *closed triangles*), it follows that binding of 7-HC to the apo SULT1A1 did not occur under these conditions. The titration of PAP into enzyme pre-mixed with 7-HC (Fig. 3, *closed circles*) produced a ΔH predicted by adding the values of the PAP-only and 7-HC into SULT:PAP titrations. This conservation of energy indicated that 7-HC did not bind to SULT1A1 unless PAP was already docked.

Table 1. Thermodynamic parameters of bSULT1A1 binding of PAP and 7-HC[a]

Sample	Titrant	K_d *μM*	N[b]	ΔH *kcal/mol*	ΔS *cal/mol/K*	ΔS x 298K *kcal/mol*
SULT	PAP	0.062 (0.012)[c]	0.651 (0.049)	-14.28 (0.54)	-14.8 (2.0)	-4.43
SULT	7-HC	ND[d]	ND	ND	ND	
SULT:PAP[e]	7-HC	1.45 (0.26)	0.507 (0.072)	-13.0 (1.6)	-16.7 (5.8)	-5.0
SULT+7-HC	PAP	0.091 (0.036)	0.521 (0.043)	-27.4 (2.5)	-59.8 (9.1)	-17.8

[a]All titrations were conducted at 25 ℃ (Methods). See Fig. 3 for representative analyses.

[b]N = mol bound titrant per mol bSULT1A1 subunit

[c]Values in parenthesis are standard deviations of 3-4 determinations.

[d]ND, not determined due to absence of signal

[e]The primary ligand was 1.5x SULT subunit concentration

3.4. Differential Scanning Fluorimetry (DSF)

The binding of ligands commonly increases protein thermostabilities, and this can be observed by following denaturation in the presence of an indicator dye (Sypro orange) that detects hydrophobic domains that become exposed. We were therefore curious if DSF might reveal binding of either PCP or 7-HC to SULT1A1 in the absence of PAP. The apo protein exhibited a T_m of 52 ℃, and this was not affected by either 20 μM (not shown) or 200 μM 7-HC (Fig. 4B). PCP alone (10 μM) possibly destabilized the protein very slightly, an effect attributable to non-specific phenol-induced structural destabilization. The inclusion of PAP with either PCP or 7-HC increased the T_m values by 12 ℃ and 5 ℃, respectively. These results verify that binding of ligands to SULT1A1 enhances its thermostability. The lack of responses to excess PCP or 7-HC alone are therefore consistent with an absence of binding of these molecules unless the PAP binding site is occupied.

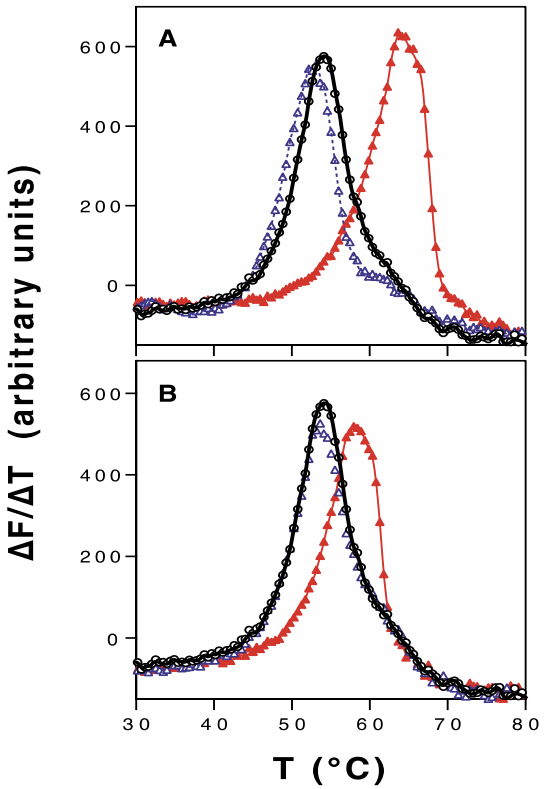

Figure 4. Evaluation of thermal stabilization of SULT1A1 by 7-HC or PCP. Each sample, performed in triplicate and averaged, contained 2.0 μM SULT1A1 subunits and 5X Sypro orange (Methods). Panel A: No additional ligands (*open circles*, thick black curve); +10 μM PCP (*open blue triangles*, dashed curve; +10 μM PAP/+10 μM PCP (*closed red triangles*, red curve). Panel B: No additional ligands (*open circles*, thick black curve); +200 μM 7-HC (*open blue triangles*); +10 μM PAP/+200 μM 7-HC (*closed red triangles*, red curve).

3.5. SULT1A1 Protease Susceptibility

We postulated that instrinsically-disordered apo bSULT1A1 might be more sensitive to proteolysis compared to the enzyme with bound ligands. Chymotrypsin was chosen due to its strong preference for aromatic side chains that are generally buried within folded proteins. Indeed, the progressive fragmentation of bSULT1A1 by chymotrypsin is hindered by PAP (Fig. 5). Although inclusion of excess 7-HC itself had no effect, its co-binding with PAP augmented the PAP-induced resistance to the protease. Densitometry verified this visual impression. The uncut SULT1A1 bands in the .0018 and .0036 mg/ml chymotrypsin incubations with both PAP and 7-HC are 17-18% more intense compared to when only PAP was present. Furthermore, the proteolytic fragments in the +/+ lanes are less intense in comparison to the +/- lanes. So although 7-HC by itself had no protective effect, its inclusion with PAP may further stabilize the conformational change induced by the nucleotide.

Exactly where chymotrypsin cleaved bSULT1A1 is unknown. Although each of the surface loops L1-3 (see below) include aromatic residues, the predicted pattern of partially digested fragments does not match what is observed (not shown). Inspection of the closed and open bSULT1A1 structures for surface aromatic residues revealed several candidate sites (Y14, Y23, W37, F210, W264, and W293). Y23 is of greatest interest, as its exposure is significantly reduced in the closed conformation compared to the postulated open state. Therefore, chymotryptic cleavage after Y23 could be impeded upon ligand binding to SULT1A1. Such hydrolysis would generate a 31.5 kDa fragment, and this matches one of the first observed cleavage products (Fig. 5). Of course there are enough additional prospective chymotryptic cleavage sites on which to propose a model consistent with the data. However, actual peptide identification will require investigation beyond the scope or purpose of this work, which was simply to determine if ligand binding affects protease sensitivity.

Although we are presenting the positive results observed with chymotrypsin, successful experiments were also conducted with neutral protease (dispase). This protease has preference after L and F residues. Again it was observed that PAP binding protected the SULT1A1 from proteolysis, whereas the phenolic ligand was not effective (not shown).

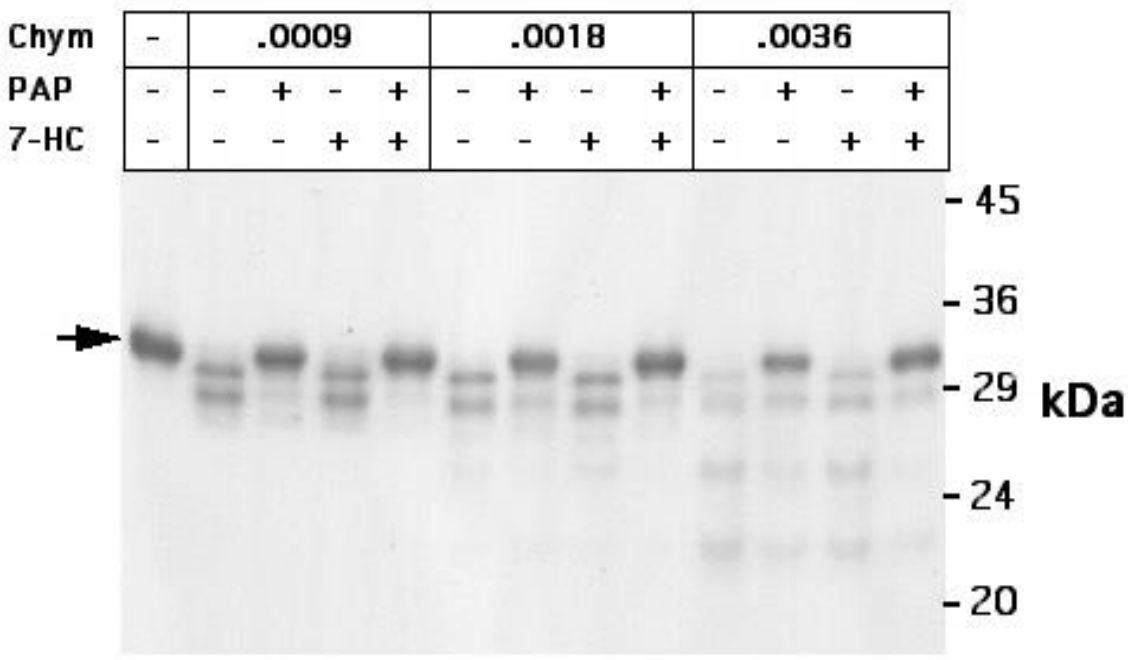

Figure 5. Effects of PAP and 7-HC on the susceptibility of bSULT1A1 to cleavage by α-chymotrypsin. The enzyme samples (0.20 mg/ml, 5.8 μM) included 50 μM PAP and/or 7-HC as indicated, followed by 30 min exposures to the protease at the indicated concentrations (mg/ml). Each lane of the SDS-PAGE gel received 4 μg bSULT1A1 protein after heat denaturation in the presence of dodecyl sulfate and 2-mercaptoethanol (Methods). The *arrow* points at undigested bSULT1A1.

3.6. Cysteine Chemical Reactivities

The bovine SULT1A1 contains three cysteinyl residues (C70, C168, C287) that are not obviously within the ligand binding domains of the protein (see below). It was previously reported that PAPS binding decreased the reaction rates of two of these residues with DTNB [38], presumably due to conformational changes that restricted cysteine availability. Therefore, we decided to conduct this reaction again, but also in the presence of excess 7-HC. Fig. 6 shows representative reaction progress curves of SULT1A1 with a pseudo first-order concentration of DTNB (Methods). As previously reported, the apo enzyme reacted with DTNB in two apparent phases, and the curve was adequately modeled with two first-order processes. This was not affected by the inclusion of 200 μM 7-HC, an amount in 20-fold excess to the protein. Inclusion of excess PAP, however, impeded the reaction as previously reported [38]. Binding of both PAP and 7-HC further slowed the reaction with DTNB, indicating additional stabilization of the protein in a "closed" conformation. This is consistent with the enhanced ΔH observed by calorimetry, which showed greater stabilization of a closed or "tight" protein conformation by 7-HC as initiated by PAP. Incomplete protection from DTNB by the ligands is explained by two factors. First, ligand binding is reversible and their inevitable release continually exposed some enzyme to the reagent as the "open" conformation was formed. Second, the anti-cooperativity of the dimer (if true) would force half of the subunits into a reactive "open" conformation. Regardless, there was no evidence from these experiments of binding of 7-HC alone to SULT1A1.

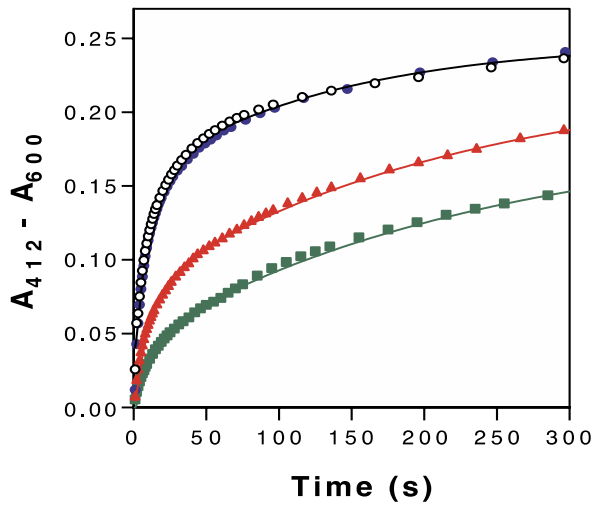

Figure 6. Effects of PAP and 7-HC on the reaction kinetics between SULT1A1 and DTNB. Reactions at pH 6.5 were initiated by mixing 100 μM DTNB into 10 μM enzyme subunits as absorbance was recorded. *Open circles* are SULT1A1 alone; *closed circles* included 200 μM 7-HC; *triangles* included 60 μM PAP; *squares* included both PAP and 7-HC. The smooth curves were calculated using summed first-order kinetics terms (*Methods*).

3.7. Molecular Modeling Explains Cysteine Reactivity Changes

Although the structure of bSULT1A1 has not been determined directly, its extensive identity and similarity to the human enzyme have allowed the modeling of its structure [12,36]. We have also applied lessons learned from other SULTs regarding conformational changes between the determined ligand-bound states and the free or apo form (Methods). The largest oscillating structural domain, encoded by the sixth exon in all SULTs, is the 30 residue loop (L3) that covers both the nucleotide and acceptor binding sites (Fig. 7). Importantly, the boundaries of this lid are nearest the PAP(S) pocket, and these locations have a mechanistic consequence. Namely, the binding of nucleotide initiates closure of L3, modeling of which has suggested flexion of its distal portion in a kinetically distinct event [15]. Recent molecular dynamics calculations have supported this view [28]. Two shorter loops, L1 and L2 (Methods, Fig. 7), exist near the distal end of L3. The motions of these three domains appear to control binding and release of acceptor site ligands [28]. The variable placements of these domains, along with some side chain conformations in the binding pocket, account for the abilities of SULTs to accommodate a spectrum of ligands [27].

We sought to understand if the movements of L1-3 might account for the ligand-induced changes in cysteine chemical reactivities of bSULT1A1 (Fig. 7). In the closed conformation C70 and C287 are barely visible when the structure is examined in space filling (Fig. 7C) or molecular surface modes (not shown), and C168 is entirely buried. In contrast, the open or apo state reveals very significant C168 exposure (Fig 7B, D), whereas no obvious changes in C70 and C287 exposures were observed. Previous work using site-directed mutant enzymes has shown that C168 accounts for the rapid phase of reaction with DTNB [26]. C168, which is unique to the bSULT1A1, is located on a knuckle that separates two helices. Interestingly, we noticed that opening of L3 alone did not expose C168 (not shown), but rather the opening of L2 dramatically revealed the thiol. Movement of L1 did not affect C168 exposure. Therefore, since binding of PAP alone was sufficient to impede the rapid phase of DTNB reaction with bSULT1A1 (Fig. 6), it follows that closure of L3 is coupled to closure of L2. Recent molecular dynamics simulations have suggested a positive correlation between L2 and L3 motions [37], thus substantiating this proposed L2/L3 coupling.

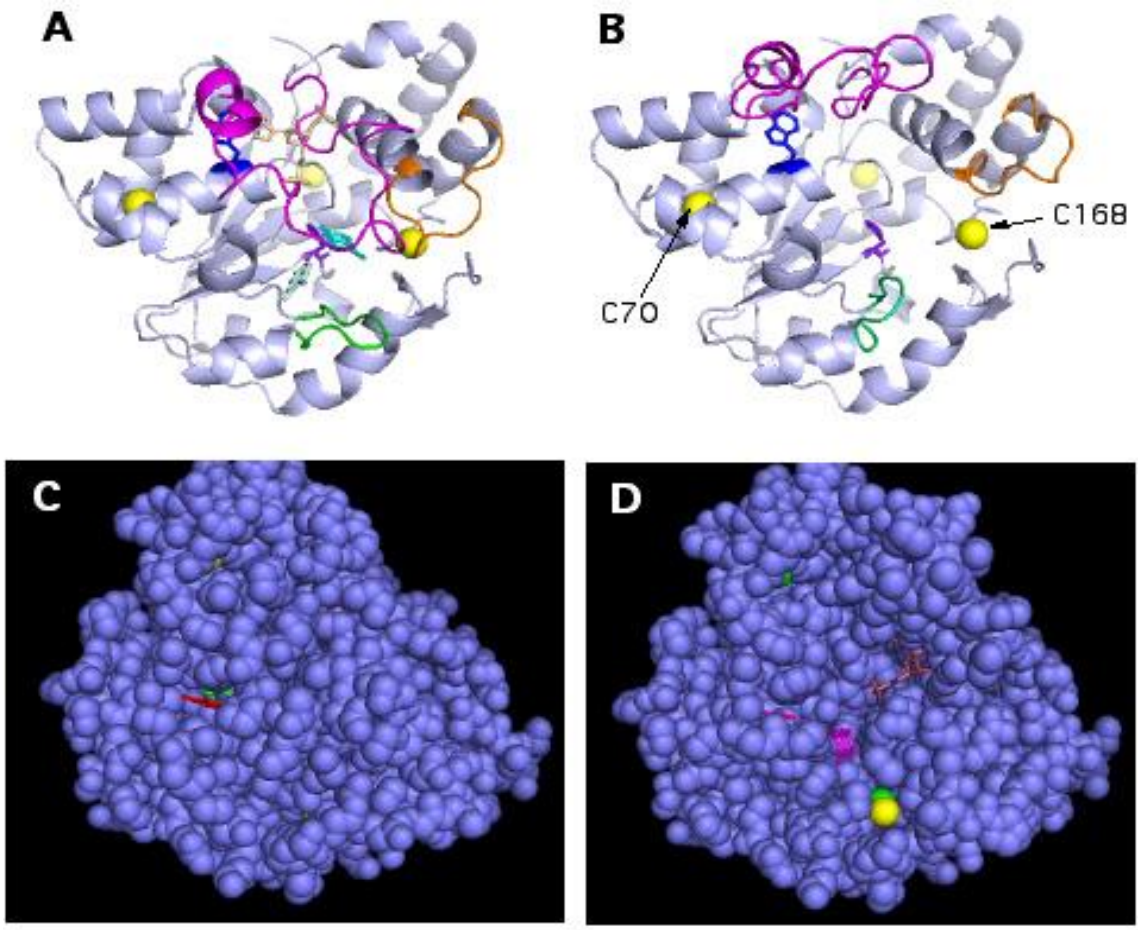

Figure 7. Modeling of bSULT1A1 structures and cysteine exposures. The ligand-bound state (A, C) is based on the hSULT1A1 structure (PDB 3u3o) with one PAP and two hydroxycoumarin molecules bound per subunit (Methods). The opened model (B, D) was empirically generated (Methods) by flexing the surface loop domains L1 (teal), L2 (orange), and L3 (magenta). The viewpoints of the ribbon models are not the same as the space-filling models. W53 and H108 (sticks in A, C) are blue and purple, respectively. PAP, inner or catalytic HC, and outer or non-catalytic HC are colored brick (A, D), teal (A) or magenta (D), and light teal (A) or red (C, D), respectively. The pale yellow sphere, located on the back side of the cartoon models (A, B), is the sulfur atom of C287. The unlabeled yellow atom in panel D is the sulfur of C168. Ligands were left in place in the open space-filling model (D) for reference and discussion.

3.8. Re-evaluation of Initial Rate Kinetics Data

We previously reported the effects of site-directed mutagenesis of the PAPS-binding site residue, W53 [33]. Trimming away the indole ring decreased the pi-pi overlap with the adenine ring of the nucleotide substrate, which decreased the apparent affinity and catalytic efficiency. The data were evaluated according to a random bisubstrate scheme, owing in part to reports that such a model was most consistent with other investigations of SULT catalysis [30,45]. However, in light of the experiments presented here we questioned whether the kinetic data would be more adequately analyzed using an ordered scheme. Therefore, we re-evaluated all the kinetic data in our previous work. While a rapid equilibrium model was considered, that would only be sound if the actual rate of sulfuryl transfer within the SULT:PAPS:7-HC complex was the rate limiting step [41]. But investigations of other SULTs have indicated that the limitation of catalytic turnover is the release of the nucleotide product, PAP. Therefore, using steady-state derivation was considered a more rigorous approach, and the kinetic data were evaluated anew with (3) (Methods). Global numerical fitting for the wild type and each of the three W53 mutant enzymes converged very quickly compared to fitting with the random model (Methods). The results are summarized in Table 2. The updated parameters still support the conclusion that the highly-conserved W53 contributes very significantly to the catalytic function of SULT1A1 and presumably all other SULTs. Note that K_{ia} is the theoretical dissociation constant for PAPS with which ΔG of binding is related (-RT x *ln*K). Using the values of K_{ia} for the WT, and either W53L or W53A enzymes, we estimate an average $\Delta\Delta G$ of 0.9 kcal/mol (3.8 kJ/mol) for the contribution of W53 to the binding of PAPS.

Table 2. Updated effects of W53 mutations on bSULT1A1 kinetic parameters

	WT	W53Y	W53L	W53A
K_{ia} (μM)	0.349 (0.074)[a]	0.913 (0.055)	1.85 (0.37)	1.39 (0.26)
K_{mA} (μM)	1.15 (0.06)	1.99 (0.07)	10.2 (0.7)	10.3 (0.4)
K_{mB} (μM)	0.649 (0.021)	2.84 (0.04)	4.67 (0.12)	2.69 (0.05)
k_{cat} (min^{-1})	9.10 (0.08)	12.54 (0.08)	9.42 (0.11)	4.97 (0.04)
k_{cat}/K_{mA} $(\mu M\text{-}min)^{-1}$	7.91	6.30	0.92	0.48

[a]Values in parentheses are the standard errors.

4. Discussion

The overall purpose of this project was to obtain evidence for the most appropriate model to describe binding of nucleotide (PAP/S) and a simple phenol (7-HC) to the bovine SULT1A1. This enzyme is 83.7% identical and 94% similar to the human SULT1A1 [33], and so the results of this work are likely relevant to other studies. We began by reconsidering intrinsic fluorescence responses to these ligands (Fig. 1), an approach used with other SULTs [13,25,27,32,46]. Indeed, fluorimetric titrations of some SULTs have been interpreted as proving random ligand binding [17,32]. In our case, the fluorescence responses were co-dependent on occupation of both the nucleotide and phenol binding sites (Fig. 1). What at first appeared to be quenching of bSULT1A1 intensity by 7-HC, suggesting direct binding of the phenol, was instead a non-specific inner filter effect. This brought into question whether other reports of SULT ligand binding and kinetics might have suffered such an artifact. For example, fluorimetric titrations of human SULT1A1 with hydroxytamoxifen and 1-hydroxypyrene, both strong UV chromophores, may have come to erroneous conclusions [17]. Therefore, additional methods were necessary for this investigation.

Equilibrium dialysis revealed the inability of SULT1A1 to bind 7-HC in the absence of nucleotide (Fig. 2). Although it could be argued that greater than 100 μM 7-HC would be needed for binding to a putative very low affinity state, doing so would exceed meaningful physiological exposure. The concavity of the Scatchard analysis indicated multiple 7-HC binding phases to the SULT1A1:PAP complex, with the initial K_d of 0.7 μM and a stoichiometry of one ligand per enzyme dimer. This matches previous fluorimetric titrations that followed Förster energy transfer from excited tryptophanyls to bound 7-HC [16], a phenomenon that also required PAP. The weak binding phase of the Scatchard plot (K_d of about 40 μM) was also PAP-dependent, and visual extrapolation suggested total binding of two 7-HC per SULT1A1 subunit. This agrees with a crystallography report of human SULT1A1 with two hydroxycoumarins per PAP-saturated subunit [39].

To our knowledge ITC has not been applied in previous investigations of SULTs, and we are only aware of its application to the mouse heparan sulfate 3-O-sulfotransferase (3-OST) [47]. Our results indicated binding order (Fig. 3, Table 1). No enthalpic signal was observed when titrating the apo SULT1A1 with 7-HC, but titration with PAP was exothermic and easily fit with a single binding site model. Subsequent titration of SULT1A1:PAP then revealed 7-HC binding. Both PAP and 7-HC exhibited about 0.5 bound ligands per subunit and thus 1 bound per dimeric SULT. Summation of ΔH values of the PAP-into-SULT1A1 titrations, with the 7-HC-into-SULT1A1:PAP titrations, matches the ΔH of titrating the SULT plus 7-HC mixture with PAP (Table 1). Furthermore, $K_{d,\ PAP}$ x $K_{d,\ 7HC}$ = 0.090 μM matches the apparent $K_{d,\ PAP}$ of 0.091 μM determined when titrating the mixture of SULT1A1 plus 7-HC (Table 1). So both ΔH and ΔG are accounted for and thus preclude a hypothetical SULT1A1:7-HC complex.

A proposal [45] that binding of PAP(S) induces closure of L3, followed by preferential binding of smaller acceptors through a size-selecting pore, may conflict with our calorimetry results. First, the ΔH values for binding PAP and for 7-HC are nearly equivalent (Table 1). If binding of 7-HC was a simple process of entering a pore, then its ΔH would be much less than for binding of PAP. Second, the losses of entropy for each ligand binding are equivalent within error (Table 1). ΔS is due to changes in the solvated ligand structures, combined with the SULT1A1 structural changes from disordered loops to a closed ordered state (Fig. 7). Based on relative sizes, the entropic contribution of the loops would exceed those of the ligands. Therefore, if binding of PAP(S) induced complete loop closure, then the majority of ΔS would be due to nucleotide binding. But this is contrary to what is observed, and instead partial closure of L3 onto PAP(S) seems more tenable. This is consistent with modeling calculations that indicated flexion of L3 approximately

midway between the loop bases and its apex [13,48].

The absence of 7-HC effects on SULT1A1 thermostability (Fig. 4), protease susceptibility (Fig. 5), or cysteine reactivity (Fig. 6) contraindicate its direct binding to the enzyme. In contrast, PAP *does* affect these properties and this verifies its binding in the absence of the phenol. Our DSF results (Fig. 4) compare well to more extensive tests of human SULTs for ligand stabilization by thermal aggregation, a method not requiring an indicator dye [49]. In that work numerous phenolic compounds, not including coumarins, had no effects on the T_m of SULT1A1 up to 1000 μM, and it was concluded that SULT1A1 is first primed by PAP to subsequently bind phenols.

Molecular modeling of the bovine SULT1A1 was informative (Fig. 7). For example, whereas cysteinyl thiols are occluded in the ligand-bound or "closed" conformation, opening of the flexible loops L1-3 revealed exposure of C168. Cysteine at this location is not conserved, so attempting the DTNB reactivity experiment with other SULTs from other species is unlikely to reveal the same ligand dependency reported here (Fig. 6). Pre-incubation of bSULT1A1 with excess 7-HC alone had no effect on the DTNB reaction (Fig.6), indicating no closure of L2 and possibly L3. Although it is possible that 7-HC alone bound to the apo SULT1A1 without inducing conformational changes, the more obvious conclusion that is consistent with other experiments reported herein is that 7-HC did not bind effectively to the apo enzyme. Inclusion of 7-HC with PAP augmented the impairment of the fast phase of DTNB reaction, which could be due to additional stabilization of L3 and L2 closure initiated by nucleotide binding.

A possible role of L1 movement was suggested by our empirical modeling. The closed conformation of SULT1A1 can accommodate two phenols per subunit [6,39] (Fig. 7A). This fact was previously used to devise a steady state kinetic model for substrate inhibition, commonly observed with SULTs [6]. However, the physical mechanism behind the model was unclear. We observed (Fig. 7) that A86 of L1 clashes with the outer non-catalytic hydroxycoumarin when L1 was flexed "open". This might account for the much weaker binding of the second phenol to the outer location. As a corollary, if the second phenol *is* bound, then opening of L1 would be impeded. Holding L1 closed would likely hinder dissociation of sulfated product and thus decrease the rate of catalytic turnover. Another mechanism of SULT substrate inhibition may involve the binding of fresh acceptor substrate before release of PAP, thus forming a dead end ternary complex [25,50]. These two models of substrate inhibition are not mutually exclusive.

The inhibitory effect of ligand binding on SULT susceptibility to proteolysis (Fig. 5) is a new observation. The intrinsically-disordered apo-SULT1A1 was readily attacked by chymotrypsin. Inclusion of excess 7-HC did not impede cleavage, which is attributable to absence of binding to the apo-enzyme. In contrast, PAP±7-HC effected enough structural change to hinder chymotrypsin site access. The protection was not complete, which is expected if the enzyme was in a dynamic equilibrium with some apo form. Given enough time or protease excess, therefore, complete degradation would occur even in the presence of ligands. A subtle feature of these experiments is the absence of approximately 50% rapid proteolysis in the presence of PAP±7-HC. This was predicted based on the proposed model of SULT structure and function of anti-cooperativity [16], in which ligand binding to one subunit of the dimer induces the relaxation and opening of the adjoining subunit. If this were correct, then the samples with ligand would have exhibited a rapid 50% fragmentation by chymotrypsin. But this was not observed (Fig. 5). Another proposed structural model of SULT function is PAPS-induced opening of *both* subunits [17], but this is contrary to these and other observations. Finally, the protection of SULT1A1 by bound nucleotide suggests a biological role in the longevity of the protein, if intracellular proteases and other protein turnover mechanisms are affected by its structure. This hypothesis creates a new line of investigation that may uncover important features that regulate SULT1A1 and other members of this enzyme family.

5. Conclusions

Evidence for direct binding of 7-HC to the bovine SULT1A1 was sought using six distinct methods. Protein fluorescence, equilibrium dialysis, titration calorimetry, differential scanning fluorimetry, protease susceptibility, and thiol reactivity all failed to reveal binding and/or structural changes of the apoenzyme to the phenol. Initial binding of PAP was required for each method to then show an effect attributable to binding of 7-HC. Numerical fitting of previous initial rate data using an ordered steady state model, with PAPS as the leading substrate, was an improvement compared to a random scheme. Although this SULT1A1 behaves in an ordered manner with 7-HC as the acceptor site ligand, this does not preclude the possibility that other ligands will bind to the enzyme in the absence of nucleotide. Some approaches taken here may be helpful when investigating other members of the SULT superfamily.

Abbreviations

SULT: sulfotransferase
PAPS: 3'-phosphoadenosine-5'-phosphosulfate
PAP: adenosine- 3',5'-bisphosphate
7-HC: 7-hydroxycoumarin
PCP: pentachlorophenol
DSF: differential scanning fluorimetry
ITC: isothermal titration calorimetry
DTNB: 5,5'-dithiobis (2-nitrobenzoic acid)
PAGE: polyacrylamide gel electrophoresis

Acknowledgements

We thank the many students of the Alma College Biochemistry program for their efforts during the preliminary stages of this investigation, but most notably Christy Robinson, Jason Alkirwi, and Caleb Woods. We also acknowledge the untold benefactors who helped create the campus Science Initiative Fund. This research did not receive any specific grant from funding agencies in the public, commercial, or not-for-profit sectors.

Conflicts of Interest

None.

REFERENCES

[1] Falany C.N., Wilborn T.W., "Biochemistry of cytosolic sulfotransferases involved in bioactivation," Adv. Pharm., vol.27, pp.301-329, 1994.

[2] Coughtrie M.W.H., "Sulfation through the looking glass - recent advances in sulfotransferase research for the curious," Pharmacogen. J., vol.2, pp.297-308, 2002.

[3] Suiko M., Kurogi K., Hashiguchi T., Sakakibara Y., Liu M.-C., "Updated perspectives on the cytosolic sulfotransferases (SULTs) and SULT-mediated sulfation," Biosci. Biotech. Biochem., vol.81, pp.63-72, 2017.

[4] Gunal S., Hardman R., Kopriva S., Mueller J.W., "Sulfation pathways from red to green," J. Biol. Chem., vol.294, pp.12293-12312, 2019.

[5] Blanchard R.L., Freimuth R.R., Buck J., Weinshilboum R.M., Coughtrie M.W.H., "A proposed nomenclature system for the cytosolic sulfotransferase (SULT) superfamily," Pharmacogenetics, vol.14, pp.199-211, 2004.

[6] Gamage N.U., Duggleby R.G., Barnett A.C., Tresillian M., Latham C.F., Liyou N.E., McManus M.E., Martin J.L., "Structure of a human carcinogen-converting enzyme, SULT1A1," J. Biol. Chem., vol.278, pp.7655-7662, 2003.

[7] Barnett A.C., Tsvetanov S., Gamage N., Martin J.L., Duggleby R.G., McManus M.E., "Active site mutations and substrate inhibition in human sulfotransferase 1A1 and 1A3," J. Biol. Chem., vol.279, pp.18799-18805, 2004.

[8] Cook I., Wang T., Falany C.N., Leyh T.S., "High accuracy *in silico* sulfotransferase models," J. Biol. Chem., vol.288, pp.34494-34501, 2013.

[9] Lessigiarska I., Peng Y., Tsakovska I., Alov P., Lagarde N., Jereva D., Villoutreix B.O., Nicot A.B., Pajeva I., Pencheva T., Miteva M.A., "Computational analysis of chemical space of natural comopunds interacting with sulfotransferases," Molecules, vol.26, pp.6360, 2021.

[10] Ma G., Geng L., Lu Y., Wei X., Yu H., "Investigating the molecular mechanism of hydroxylated bromdiphenyl ethers to inhibit the thyroid hormone sulfotransferase SULT1A1," Chemosphere, vol.263, pp.128353, 2021.

[11] Hsiao Y.-S., Yang Y.-S., "A single mutation converts the nucleotide specificity of phenol sulfotransferase from PAP to AMP," Biochem., vol.41, pp.12959-12966, 2002.

[12] Beckmann J.D., Chodavarapu S., Doyle B., "Evaluation of a conserved tryptophanyl residue in donor substrate binding and catalysis by a phenol sulfotransferase (SULT1A1)," Arch. Biochem. Biophys., vol.695, pp.108621, 2020.

[13] Dajani R., Cleasby A., Neu M., Wonacott A.J., Jhoti H., Hood A.M., Modi S., Hersey A., Taskinen J., Cooke R.M., Manchee G.R., Coughtrie M.W.H., "X-ray crystal structure of human dopamine sulfotransferase, SULT1A3," J. Biol. Chem., vol.274, pp.37862-37868, 1999.

[14] Bidwell L.M., McManus M.E., Gaedigk A., Kakuta Y., Negishi M., Pedersen L., Martin J.L., "Crystal structure of the human catecholamine sulfotransferase," J. Mol. Biol., vol.293, pp.521-530, 1999.

[15] Cook I., Wang T., Almo S.C., Kim J., Falany C.N., Leyh T.S., "The gate that governs sulfotransferase selectivity," Biochemistry, vol.52, pp.415-424, 2013.

[16] Beckmann J.D., Henry T., Ulphani J., Lee P., "Cooperative Ligand Binding by Bovine Phenol Sulfotransferase," Chem.-Biol. Interact., vol.109, pp.93-105, 1998.

[17] Tulik G.R., Chodavarapu S., Edgar R., Giannunzio L., Langland A., Schultz B., Beckmann J.D., "Inhibition of bovine phenol sulfotransferase (bSULT1A1) by CoA thioesters," J. Biol. Chem., vol.277, pp.39296-39303, 2002.

[18] Beckmann J.D., Burkett R.J., Sharpe M., Giannunzio L., Johnston D., Abbey S., Wyman A., Sung L., "Spectrofluorimetric analysis of 7-hydroxycoumarin binding to bovine phenol sulfotransferase," Biochim. Biophys. Acta, vol.1648, pp.134-139, 2003.

[19] Wang T., Cook I., Leyh T.S., "3'-Phosphoadenosine 5'-phosphosulfate allosterically regulates sulfotransferase turnover," Biochemistry, vol.53, pp.6893-6900, 2014.

[20] Petrochenko E.V., Pedersen L., Borchers C.H., Tomer K.B., Negishi M., "The dimerization motif of cytosolic sulfotransferases," FEBS Letters, vol.490, pp.39-43, 2001.

[21] Hughes K.L., Dopke J.A., Beckmann J.D., "Design and properties of mutant sulfotransferases for heterodimerization," 237th ACS National Meeting, Salt Lake City, UT, Biol. 169, 2009.

[22] Schauss S.J., Henry T., Palmatier R., Halvorson L., Dannenbring R., Beckmann J.D., "Characterization of Bovine Tracheobronchial Phenol Sulfotransferase cDNA and Detection of mRNA Regulation by Hydrocortisone," Biochem. J., vol.311, pp.209-217, 1995.

[23] Yang Y.-S., Marshall A.D., McPhie P., Guo W.A., Xie X., Chen X., Jakoby W.B., "Two Phenol Sulfotransferase Species from One cDNA: Nature of the Differences," Protein Expression Purif., vol.8, pp.423-429, 1996.

[24] Laemmli U.K., "Cleavage of structural proteins during the assembly of the head of the bacteriophage T4," Nature, vol.227, pp.680-685, 1970.

[25] Beckmann J.D., Frerman F.E., "Electron-transfer flavoprotein-ubiquinone oxidoreductase from pig liver: purification and molecular, redox, and catalytic properties," Biochem., vol.24, pp.3913-3921, 1985.

[26] Chodavarapu S., Hertema H., Huynh T., Odette J., Miller R., Fullerton A., Alkirwi J., Hartsfield D., Padmanabhan K., Woods C., Beckmann J.D., "Reversible Covalent Inhibition of a Phenol Sulfotransferase by Coenzyme A," *Arch. Biochem. Biophys.*, vol.457, pp.197-204, 2007.

[27] Berger I., Guttman C., Amar D., Zarivach R., Aharoni A., "The Molecular Basis for the Broad Substrate Specificity of Human Sulfotransferase 1A1," PLoS ONE, vol.6, pp.e26794, 2011.

[28] Dudas B., Toth D., Perahia D., Nicot A.B., Balog E., Miteva M.A., "Insights into the substrate binding mechanism of SULT1A1 through molecular dynamics with excited normal modes simulations," Nature Sci. Rep., vol.11, pp.13129, 2021.

[29] Segel I.H., "Biochemical Calculations, Chapter 4: Enzymes," *Wiley*, New York, pp. 293-295, 1976.

[30] Duffel M.W., Jakoby W.B., "On the Mechanism of Aryl Sulfotransferase," *J. Biol. Chem.*, vol.256, pp.11123-11127, 1981.

[31] Zhang H., Varmalova O., Vargas F.M., Falany C.N., Leyh T.S., "Sulfuryl transfer: the catalytic mechanism of human estrogen sulfotransferase," *J. Biol. Chem.*, vol.273, pp.10888-10892, 1998.

[32] Sun M., Leyh T.S., "The human estrogen sulfotransferase: a half-site reactive enzyme," *Biochem*., vol.49, pp.4779-4785, 2010.

[33] Wang T., Cook I., Falany C.N., Leyh T.S., "Paradigms of sulfotransferase catalysis," *J. Biol. Chem.*, vol.289, pp.26474-26480, 2014.

[34] Mulder G.J., Scholtens E., "Phenol Sulphotransferase and Uridine Diphosphate Glucuronyltransferase from Rat Liver in vivo and in vitro," *Biochem*. J., vol.165, pp.553-559, 1977.

[35] Edavettal S.C., Lee K.A., Negishi M., Linhardt R.J., Liu J., Pedersen L.C., "Crystal structure and mutational analysis of heparan sulfate 3-O-sulfotransferase isoform 1," *J. Biol. Chem.*, vol.279, pp.25789-25797, 2004.

[36] Choughule K.V., Locuson C.W., Coughtrie M.W.H., "Characterization of bovine phenol sulfotransferases: evidence of a major role for SULT1B2 in the liver," *Xenobiotica*, vol.45, pp.495-502, 2014.

[37] Dash R., Ali C., Dash N., Azad A.K., Hosen S.M.Z., Hannan A., Moon I.S., "Structural and dynamic characterizations highlight the deleterious role of SULT1A1 R213H polymorphism in substrate binding," *Int. J. Mol. Sci.*, vol.20, pp.6256, 2019.

[38] Cook I., Wang T., Falany C.N., Leyh T.S., "A nucleotide-gated molecular pore selects sulfotransferase substrates," *Biochem*., vol.51, pp.5674-5683, 2012.

[39] Tibbs Z.E., Rohn-Glowacki K.J., Crittenden F., Guidry A.L., Falany C.N., "Structural plasticity in the human cytosolic sulfotransferase dimer and its role in substrate selectivity and catalysis," *Drug Met. Pharm.*, vol.30, pp.3-20, 2015.

[40] Pennings E.J.M., Vrielink R., van Kempen G.M.J., "Kinetics and Mechanism of the Rat Brain Phenol Sulphotransferase Reaction," *Biochem. J*., vol.173, pp.299-307, 1978.

[41] Whittemore R.M., Pearce L.B., Roth J.A., "Purification and Kinetic Characterization of a Dopamine-sulfating Form of Phenol Sulfotransferase from Human Brain," *Biochem.*, vol.24, pp.2477-2482, 1985.

[42] Whittemore R.M., Pearce L.B., Roth J.A., "Purification and Kinetic Characterization of a Phenol-sulfating Form of Phenol Sulfotransferase from Human Brain," *Arch. Biochem. Biophys.*, vol.249, pp.464-471, 1986.

[43] Barnes S., Waldrop R., Crenshaw J., King R.J., Taylor K.B., "Evidence for an ordered reaction mechanism for bile salt: 3'phosphoadenosine- 5'-phosphosulfate: sulfotransferase from rhesus monkey liver that catalyzes the sulfation of the hepatotoxin glycolithocholate," *J. Lipid Res.*, vol.27, pp.1111- 1123, 1986.

[44] Banerjee R.K., Roy A.B., "Kinetic studies of the phenol sulphotransferase reaction," *Biochim. Biophys. Acta*, vol.151, pp.573-586, 1968.

[45] Vakiani E., Luz J.G., Buck J., "Substrate specificity and kinetic mechanism of the insect sulfotransferase, retinol dehydratase," *J. Biol. Chem.*, vol.273, pp.35381-35387, 1998.

[46] Pi N., Hoang M.K., Gao H., Mougous J.D., Bertozzi C.R., Leary J.A., "Kinetic measurements and mechanism determination of Stf0 sulfotransferase using mass spectrometry," *Analyt. Biochem.*, vol.341, pp.94-104, 2005.

[47] Tyapochkin E., Cook P.F., Chen G., "Isotope exchange at equilibrium indicates a steady state ordered kinetic mechanism for human sulfotransferase," *Biochem.*, vol.47, pp.11894-11899, 2008.

[48] Tyapochkin E., Cook P.F., Chen G., "para-Nitrophenyl sulfate activation of human sulfotransferase 1A1 is consistent with intercepting the E-PAP complex and reformation of E-PAPS," *J. Biol. Chem.*, vol.284, pp.29357-29364, 2009.

[49] Cook I., Wang T., Almo S.C., Kim J., Falany C.N., Leyh T.S., "Testing the sulfotransferase molecular pore hypothesis," *J. Biol. Chem.*, vol.288, pp.8619-8626, 2013.

[50] Allali-Hassani A., Pan P.W., Dombrovski L., Najmanovich R., Tempel W., Dong A., Loppnau P., Martin F., Thonton J., Edwards A.M., Bochkarev A., Plotnikov A.N., Vedadi M., Arrowsmith C.H., "Structural and chemical profiling of the human cytosolic sulfotransferases," *PLoS Biol.*, vol.5, pp.1063-1078, 2007.

[51] Lee K.A., Fuda H., Lee Y.C., Negishi M., Strott C.A., Pedersen L.C., "Crystal structure of human cholesterol sulfotransferase (SULT2B1b) in the presence of pregnenolone and 3'-phosphoadenosine 5'-phosphate," *J. Biol. Chem.*, vol.278, pp.44593-44599, 2003.